Charge Transfer Process Determines Ultrafast Excited State Deactivation of Thioflavin T in Low-Viscosity Solvents

Vitali I. Stsiapura* and Alexander A. Maskevich

Department of Physics, Yanka Kupala State University, Grodno 230023, Belarus

Sergey A. Tikhomirov and Oleg V. Buganov

B.I. Stepanov Institute of Physics, National Academy of Sciences of Belarus, Minsk 220072, Belarus

Received: June 6, 2010; Revised Manuscript Received: July 12, 2010

Here we provide first direct experimental results about photoinduced TICT-state formation for Thioflavin T (ThT). In this work, femtosecond transient absorption spectra dynamics for ThT, dissolved in low-viscosity solvents (water, ethanol, 2-propanol, butanol) was investigated. It was found that decay lifetime of fluorescent LE-state for ThT in low-viscous solvents does not exceed 12 ps, and its value correlates well with rising time of the absorption band at 470 nm. It indicates that LE-state of ThT initially formed upon photoexcitation is quite rapidly converted to a transient state characterized by absorption at 470 nm. We associate this emerging intermediate state with nonfluorescent TICT-state of the dye. Rate of LE → TICT process significantly depends on viscosity and is comparable to the rate of solvent relaxation resulting in time-dependent Stokes shift of ThT stimulated emission band. TICT-state deactivation was found to be also viscosity dependent and its lifetime changed from 3.8 ± 0.1 ps (in H_2O) to 360 ± 60 ps (in butanol). It was proposed that a nonradiative deactivation process proceeds through a conical intersection between TICT(S_1') and S_0 energy levels. The results obtained confirm the earlier proposed model that twisted internal charge transfer process takes place in the excited state of the dye and that ThT behaves as a molecular rotor (Stsiapura, V. I.; Maskevich, A. A.; Kuzmitsky, V. A.; Uversky, V. N.; Kuznetsova, I. M.; Turoverov, K. K. *J. Phys. Chem. B* **2008**, *112*, 15893−15902).

Introduction

Formation and deposition of amyloid fibrils, insoluble filamentous protein aggregates, in organism tissues are closely related to several human diseases (neurodegenerative Alzheimer's and Parkinson's diseases, cataract, etc.).[1−8] Understanding amyloid fibrillation in detail is essential for development of strategies to interrupt pathological processes and overcome neurodegenerative disorders.[1,9] Therefore, versatile and reliable methods to determine amyloid fibrils content and monitor fibrillation are of great importance.[9]

One of the most frequently used methods of amyloid fibrils detection is based on the characteristic changes in thioflavin T (ThT) fluorescence intensity upon binding of this dye to amyloid fibrils.[10−17] Fluorescence quantum yield (QY) of nonbound ThT is very low ($\sim 10^{-4}$),[18] and aqueous solutions of the dye are practically nonfluorescent. It has been reported that interaction of this probe with proteins in native or unfolded states results in very slight alteration of ThT emission intensity that can usually be neglected.[10,12,19] However, upon binding to amyloid fibrils its emission intensity grows significantly by ∼3 orders as deduced from fluorescence decay lifetime change.[20]

In the recent review[9] two models explaining selective enhancement of ThT fluorescence in the presence of amyloid fibrils have been chosen as the most plausible (so-called *excimer* and *molecular rotor* models). According to the excimer model,[21−23] change of ThT emission intensity upon incorporation is attributed to formation of highly fluorescent excimers from the dye molecules in cavities of appropriate size inside amyloid fibrils. However, this model cannot satisfactorily explain the appearance of an induced circular dichroism signal in the absorption band of ThT upon its incorporation into fibrils.[24,25] Recent near-field scanning optical microscopy studies of single amyloid fibrils stained with ThT have demonstrated that the dye is bound in a monomeric form and that its molecular axis is oriented parallel to the axis of amyloid fibril.[26] These data as well as results of the studies of ThT binding to fibril-like PSAM scaffolds[27] are in good correspondence with the model proposed earlier by Krebs[28] that ThT embeds into the β-sheet grooves running along the fibrils, and growth of fluorescence intensity is related to increased rigidity of the probe microenvironment.

Photophysical studies of ThT in solvents of different viscosity[18,29,30] and in confined media[31,32] reveal that a high local microviscosity is the main factor responsible for the enhancement of ThT fluorescence. It has been proposed that twisted internal charge transfer (TICT), accompanied by torsional motion of benzothiazole and dimethylaminobenzene rings, takes place in the excited state of ThT,[30,33,34] resulting in nonfluorescent TICT-state formation (Figure 1). The rate of this process is mainly controlled by viscosity (or rigidity) of the probe microenvironment, and ThT behaves as a molecular rotor.[29,30,33−36]

In nonviscous media, twisting of ThT fragments practically is not restricted, and the charge transfer process introduces a fast nonradiative decay channel, resulting in strong quenching of ThT emission and shortening of fluorescence decay lifetime. For example, average lifetime of the emissive locally excited (LE) state for nonbound ThT in aqueous solution has been estimated to be ∼1 ps.[20,31,37] Under these conditions major part

* To whom correspondence should be addressed. Phone: +375-152-743414. Fax: +375-152-731910. E-mail: stepuro@grsu.by.

10.1021/jp105186z
Published on Web 07/28/2010

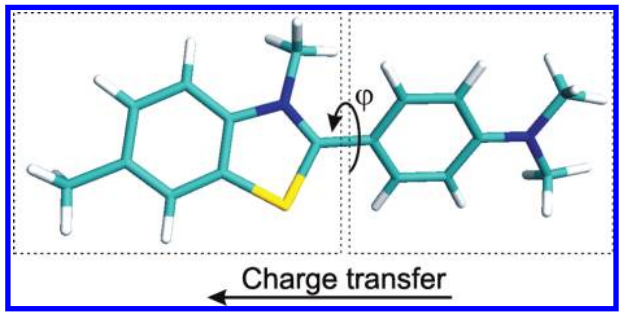

Figure 1. Scheme of photoinduced twisted internal charge transfer in Thioflavin T cation. S, C, and N atoms are shown in yellow, cyan, and blue colors, respectively. Twisting fragments of benzothiazole and dimethylaminobenzene are shown in boxes.

of the excited dye molecules undergoes transition to TICT state and deactivates nonradiatively. However, in recent works[20,38] it has been reported that the charge transfer state of the dye is emissive, a suggestion that is in contrast to an earlier proposed model.[33,34] To get insight into ThT photophysics, spectral properties of the TICT state as well as dynamics of its deactivation must be explored.

In this work femtosecond transient absorption spectra dynamics for ThT, dissolved in low-viscosity solvents (water, ethanol, 2-propanol, butanol), was investigated. Here we provide first direct experimental results about photoinduced TICT-state formation for ThT, as well as data about spectral properties and deactivation dynamics of TICT-state.

Experimental Methods

Thioflavin T (ThT) of UltraPure grade quality was purchased from Anaspec (USA) and used without further purification. Spectra-grade ethanol, 2-propanol, and butanol were purchased from Sigma (USA). Bidistilled water and alcohols were used for ThT samples preparation with concentration of 50−60 μM.

Transient absorption measurements in the sub-picosecond time domain were carried out in 0.5 cm quartz cuvette using a homemade original femtosecond spectrometer, described elsewhere.[39] Briefly, the spectrometer was based on Ti:Al_2O_3 pulse pumped oscillator and a regenerative amplifier, both operating at 10 Hz repetition rate. The Ti:Al_2O_3 master oscillator was synchronously pumped with doubled output of feedback-controlled mode-locked picosecond pulsed Nd:YAG laser. The duration and energy of the pulses after the amplifier were about 150 fs and 0.5 mJ, respectively. The fundamental output of the Ti:Al_2O_3 system (tunable over the spectral range 760−820 nm, 780 nm output wavelength was set for present study) was split into two beams in the ratio 1:4. A more intense beam was passed through a controlled delay line and then was used for the generation of the second (λ_{exc} = 390 nm) harmonics of the fundamental frequency of the Ti:sapphire laser, which were utilized as exciting pulses. The second beam of fundamental frequency was used for generation of a femtosecond supercontinuum (by focusing into a 1 cm path length cell with water or into a sapphire plate), which served as the probe radiation. The continuum probe light was split with a beam splitter into two pulses (reference and signal), which were identical in intensity, and was focused on the sample by mirror optics. The spectra of both pulses after passing through the sample were recorded for every laser flash by a polychromator equipped with silicon CCD matrix and transferred to the computer. The differential optical signal ΔD (λ, Δt) is obtained as

$$\Delta D(\lambda, \Delta t) = \log(T_0/T)$$

where $T = E_{prob}/E_{ref}$ and $T_0 = E^0_{prob}/E^0_{ref}$ are energy ratios of the probe and reference pulses that have passed through the investigated sample at excitation and without it, respectively.

Typically, 30 measurements were averaged to give a wavelength-dependent signal at every time step. The transient spectra were recorded in the range of 400−800 nm with a resolution of about 1.5 nm. We estimate the absolute error for ΔD as 0.001.

The transient spectra were corrected for the group velocity dispersion of the probe pulse. The experiments were carried out at room temperature.

The instrument response function (IRF) of the spectrometer was estimated to have Gaussian shape with fwhm of 230 fs. Transient absorption kinetic curves $\Delta D(t)$ were fitted using set of exponentials convolved with the IRF function according to the following expression

$$\Delta D(t) = \sum_i \alpha_i \exp\left(-\frac{t}{\tau_i}\right) \otimes \frac{1}{\sqrt{2\pi}\sigma} \exp\left(-\frac{(t - t_0)^2}{2\sigma^2}\right)$$

where α_i and τ_i were the amplitude and lifetime of ith exponential component respectively, t_0 is the time of the probe pulse arrival, and σ is the width parameter of IRF. Deconvolution analysis was carried out on the base of Marquardt nonlinear least-squares method.[40,41]

To improve accuracy of τ_i parameters estimation the global analysis approach[42,43] was utilized, that is, a set of kinetic curves registered at different wavelengths was simultaneously fitted using exponential components with common lifetimes. Time resolution of the femtosecond spectrometer was limited mainly by the pump−probe pulse duration and was estimated as 0.1 ps.

Results and Discussion

1. Transient Absorption Dynamics for ThT in Aqueous Solution. Transient absorption spectra of ThT in aqueous solution after excitation at 390 nm are shown in Figure 2. The steady-state absorption and fluorescence spectra are also represented to show the regions where the bleaching of the sample absorption and the gain signal are expected. One can see that besides the bleaching band at 410−450 nm, related to depopulation of the ground state of ThT, and intensive gain signal in the region of 450−600 nm, corresponding to fluorescence spectrum of the dye, new absorption bands at 470 and 720 nm also contribute to the transient absorption spectra at different time delays.

Kinetic curves of transient absorption for aqueous solution of ThT at several wavelengths are shown in Figure 3. One can see that fast recovery of the bleaching signal takes place and ~90% of its magnitude at 425 nm decays during 10−15 ps. However, the signal from the gain band degrades much more rapidly within the first 1−2 ps (a similar result is observed for the absorption at 720 nm) accompanied by simultaneous rise of the absorption band at 470 nm. It indicates that locally excited (LE) state initially produced upon ThT photoexcitation is quite rapidly converted to a transient state characterized by absorption band at 470 nm. Taking into account high rate of this process we associate this emerging intermediate form with nonfluorescent TICT-state of the dye.

Transient absorption curves were fitted using set of exponentials convolved with the pump−probe correlation function.

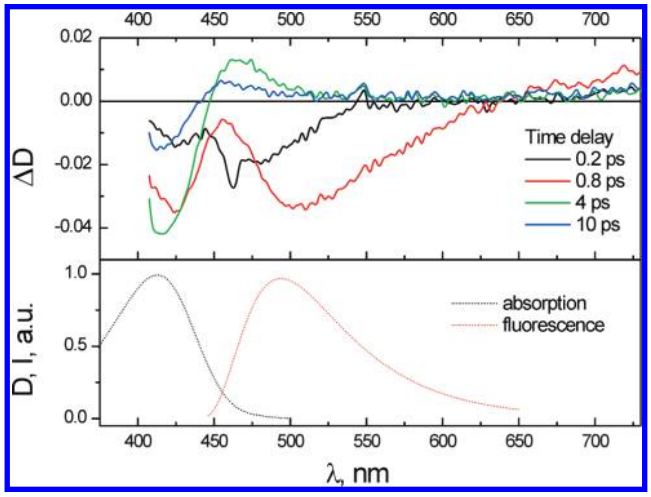

Figure 2. Transient absorption spectra of ThT in aqueous solution, registered at different time delays after excitation. $\lambda_{ex} = 390$ nm, $T = 298$ K. Shapes of steady-state absorption and fluorescence spectra are shown with dashed line. Sharp peak at 460 nm in transient spectrum for 0.2 ps time delay corresponds to induced Raman signal of the solvent.

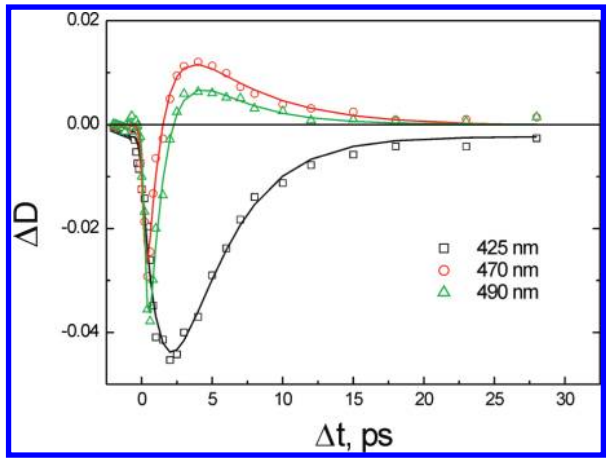

Figure 3. Kinetics of transient absorption for ThT in water at 425 nm, 470 nm, and 490 nm. $\lambda_{ex} = 390$ nm. Solid lines correspond to results of the least-squares fitting.

TABLE 1: Parameters of Transient Absorption Kinetics of ThT in H_2O[a]

λ (nm)	α_1	τ_1, ps	α_2	τ_2 (ps)
425[b]	1.00 ± 0.09	1.51 ± 0.10	-1.00 ± 0.07	3.5 ± 0.2
470	-1.00 ± 0.10	1.17 ± 0.15	0.41 ± 0.11	5.4 ± 1.1
490	-1.00 ± 0.25	1.3 ± 0.2	0.34 ± 0.23	3.7 ± 1.4
500	-1.00 ± 0.11	1.18 ± 0.16	0.22 ± 0.12	4.6 ± 1.7

[a] $T = 298$ K. $\lambda_{ex} = 390$ nm. [b] Additional long-lived component was found with $\alpha = -0.014$.

Deconvolution analysis revealed that kinetics of absorption changes in all spectral range can be described with acceptable quality using two exponential components with lifetimes $\tau_1 \sim 1.3$ ps and $\tau_2 \sim 3-5$ ps (Table 1). Only in the bleaching band range (420−425 nm) additional long-lived component ($\tau > 30$ ps) with $\alpha = -0.014$ was needed to describe temporal evolution of ΔD. To improve accuracy of parameters estimation the global analysis was utilized, that is, set of kinetic curves was simultaneously fitted using exponential components with common lifetimes. Lifetimes $\tau_1 = 1.3 \pm 0.1$ ps and $\tau_2 = 3.8 \pm 0.1$ ps were obtained using global analysis of 13 transient absorption curves. Corresponding pre-exponential factors are represented in Figure S1. It is straightforward to associate the recovered short-lived and long-lived exponential components with emissive LE and TICT states, respectively. The obtained value of LE-state lifetime is in excellent agreement with reported data of ThT fluorescence decay measurements using up-conversion technique.[20,31]

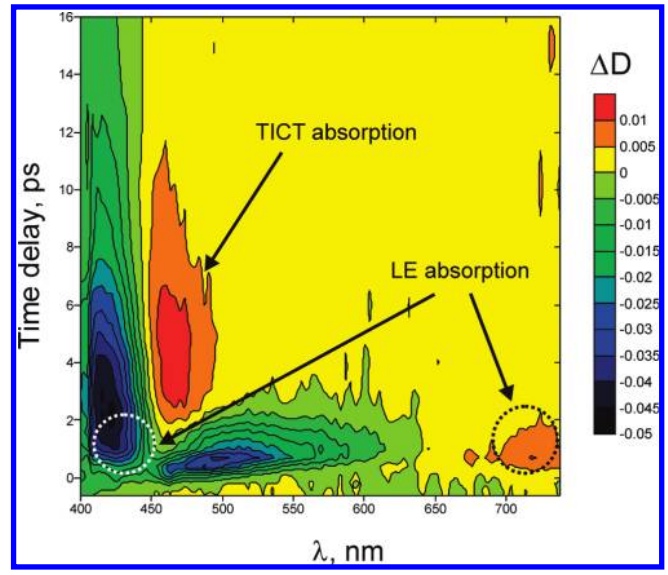

Figure 4. Image plot of transient absorption for ThT in aqueous solution as a function of wavelength and time delay after the excitation. $\lambda_{ex} = 390$ nm.

It is noteworthy that the bleaching signal recovery is not monoexponential and $|\Delta D|$ experiences rising during the first 1−2 ps after the excitation indicating presence of a hidden short-lived absorption band in this spectral region. Therefore, besides the gain signal in the range 460−600 nm and absorption band at 720 nm, LE state is also characterized by the absorption band at ∼430 nm (Figure 4).

One can see that growth of time delay after the excitation results in broadening of the gain band and noticeable shift of its position from 490−500 nm to 520−530 nm (Figure 4). Manifestation of time-dependent Stokes shift for ThT gain spectrum testifies that rates of LE → TICT transition and of solvent shell rearrangement are comparable. As a result, relaxation processes are not completed before photon emission and fluorescence of the dye has nonequilibrium character.

Time-dependent Stokes shift of ThT fluorescence in nonviscous solvents was observed earlier and associated with transition from initially excited LE-state to an emissive TICT-state on the base of TRANES data.[20] However, we suppose that presence of the isoemissive point in TRANES spectra has accidental character and that time drift of the ThT gain (or fluorescence) spectrum is caused by processes of solvent and structural relaxations in the LE-state.

It must be noted that the rate of TICT-state deactivation is very fast for ThT in aqueous solution and approaches 0.26×10^{12} s^{-1}. On the basis of quantum chemical calculations it was suggested earlier that the energy difference between the ground and TICT state levels for twisted conformation of ThT is rather small[33] and that conical intersection between the levels may occur, resulting in rapid deactivation of the excited TICT state. However, complete disappearance of the bleaching signal was not observed within the 30 ps time range after the excitation (Figure 3), indicating that ∼3−5% of the excited molecules did not return to the initial ground state and resided in a certain metastable intermediate state.

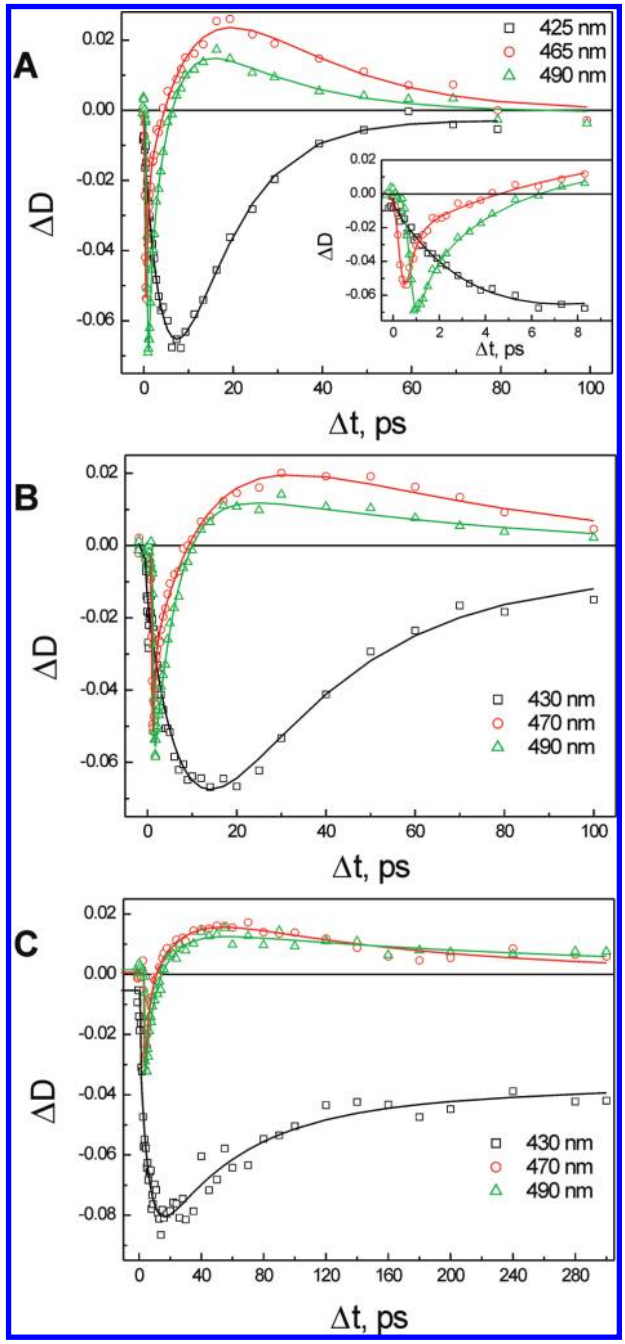

Figure 5. Transient absorption curves for ThT in ethanol (A), 2-propanol (B), and butanol (C). $\lambda_{ex} = 390$ nm. The inset of A represents time evolution of the ΔD signal for ThT in ethanol at early stages after photoexcitation. Solid lines correspond to results of the least-squares fitting.

2. Transient Absorption Dynamics for ThT in Alcohols. Similar behavior of transient absorption spectra dynamics was observed for ThT solutions in ethanol, 2-propanol, and butanol (Figure 5). Initially excited emissive LE-state, characterized by the gain band and absorption bands at ~430 and 720 nm, is rapidly converted to TICT state, however the LE → TICT transition takes more time in comparison to the case of the aqueous solution, and its rate as well as the rate of TICT-state deactivation exhibit a strong dependence on solvent viscosity. Global analysis of transient absorption data for ThT in alcohols revealed that kinetic curves in the spectral range 500−570 nm (red wing of the gain band) can be successfully fitted using biexponential model with common lifetimes (Table 2, Figure S2−S4). Values of LE- and TICT-state lifetimes, obtained after simultaneous fitting of 8−9 transient absorption curves, are shown in Table 2.

TABLE 2: Kinetic Parameters of ThT Photophysics Obtained Using Global Analysis[a]

solvent	viscosity (cP)	τ(LE) (ps)	τ(TICT) (ps)	QY[18]
H_2O	0.89	1.3 ± 0.1	3.8 ± 0.1	0.0003
ethanol	1.07	4.6 ± 0.2	28 ± 2	0.0012
2-propanol	2.13	6.4 ± 0.2	70 ± 9	0.0025
Butanol	2.66	11.8 ± 0.6	360 ± 60	0.0043

[a] $T = 298$ K, $\lambda_{ex} = 390$ nm.

An additional short-lived exponential is needed to describe time evolution of absorbance changes in the blue-wing range of the gain band (460−490 nm) in order to account for time-dependent shift of fluorescence spectrum position caused by structure and solvent relaxations. Its lifetime is much shorter than of LE-state and varies from 0.4 ps (ethanol) to 2.1 ps (butanol).

Similar to the case of an aqueous solution, the bleaching signal experiences rising within the first 5−10 ps, and its decay is nonexponential. Moreover, a significant part of the excited molecules does not return to the relaxed ground state within the time window of the spectrometer. This results in appearance of long-lived component with negative amplitude α_3 in the kinetics (Table S2 of the Supporting Information).

It is noteworthy that dependencies of τ(LE) lifetime and of fluorescence quantum yield (QY) on viscosity are very similar (Table 2) indicating that exactly LE-state is responsible for ThT fluorescence. One can see that growth of solvent viscosity from 1.07 cP (ethanol) to 2.66 cP (butanol) results in increase of LE-state (~2.5 fold) and TICT-state (~12 fold) lifetimes. Value of long-lived component amplitude α_3 is also affected by solvent viscosity (Table S2). This strong influence of surrounding medium fluidity on ThT photophysics indicates that intramolecular processes of forward (LE → TICT) and backward (TICT → S_0) charge transfers are accompanied by large alterations of the dye geometry. However, comparing LE-state lifetimes for ThT in aqueous and ethanol solutions, one can conclude that viscosity is not the only factor that determines LE → TICT transition rate and that solvent polarity as well as its protic properties also play an important role in the dye photophysics.

3. Excited States Deactivation Scheme for ThT. The results of time-resolved absorption dynamics for ThT in low-viscous media allow to improve and correct the model of the dye photophysics proposed earlier.[33,34] Quantum-chemical calculations indicated[30,33,24] that in the ground state ThT has the conformation with pretwisted benzthiazole and dimethylaminobenzene fragments ($\varphi \sim 37°$). Upon photoexcitation the dye transits to an unrelaxed LE-state responsible for ThT fluorescence (Figure 6). In addition to structural (vibrational) and solvent relaxation processes from the nonequilibrium Franck−Condon state, characterized by K_{rel}^{LE} rate and radiative transition Γ to the ground state, the efficient intramolecular charge transfer $K_{LE-TICT}$ takes place accompanied by twisting of the molecule along the C−C bond connecting the benzthiazole and dimethylaminobenzene moieties.

As it follows from quantum-chemical calculations[33] mutual rotation of ThT fragments from $\varphi = 37$ to 90° leads to the excited state energy $E(S_1)$ decrease accompanied by charge transfer between dimethylaminobenzene and benzthiazole fragments. Furthermore, oscillator strength f of the $S_0 \rightarrow S_1$ transition changes significantly upon ThT twisting ($f \sim 1$ at $\varphi = 37°$ and $f \sim 0$ at $\varphi = 90°$), which indicates that switching between

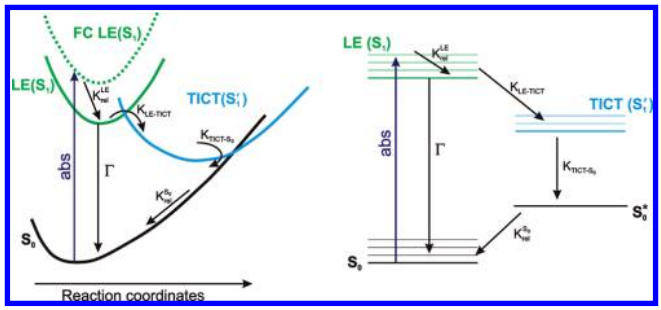

Figure 6. Excited-state deactivation scheme for ThT.

emissive LE(S_1) and nonfluorescent TICT(S_1') states takes place. Torsional angle φ between ThT fragments may be considered as a reaction coordinate for LE → TICT transition. As it was shown earlier[34] internal rotation of ThT fragments in the excited state is actually barrierless and is fully determined by the microviscosity of the dye. Indeed, mutual rotation of benzothiazole and dimethylaminobenzene moieties, which accompany intramolecular charge transfer, will perturb motion of solvent molecules in the dye vicinity, making the rate of photoinduced charge transfer process $K_{\text{LE-TICT}}$ to be viscosity-dependent.

In low-viscous media LE → TICT transition is the main route of LE-state deactivation (its rate is ~1000 times greater than radiative rate constant), and one can easily estimate $K_{\text{LE-TICT}} \approx 1/\tau(\text{LE})$.

Transient absorption data shows that the produced nonfluorescent TICT state, characterized by absorption at 470 nm (Figure 2), is deactivated rapidly to the ground state via a nonradiative transition. TICT-state deactivation rate $K_{\text{TICT-S}_0} = 1/\tau(\text{TICT})$ approaches 0.26×10^{12} s^{-1} for aqueous solution and is found to be very sensitive to solvent viscosity. On the basis of these results we suggest that TICT-state deactivation process proceeds through conical intersection between TICT(S_1') and S_0 states. Sensitivity of $K_{\text{TICT-S}_0}$ to solvent viscosity indicates that large alteration of ThT geometry takes place on the pathway to TICT/S_0 funnel. As it was reported,[44] photodynamics of molecular systems in the vicinity of conical intersection is determined by at least two reaction coordinates (for example, stretching, bending, etc.). We suppose that reaction coordinates of TICT-state deactivation process may be associated not only with twisting as in the case of LE → TICT transition but also with bending of the molecule.

After the funneling through the conical intersection, ThT has a conformation that differs significantly from the dye geometry in the relaxed ground state giving rise of structure and solvent relaxation processes with rate constant $K_{\text{rel}}^{S_0}$. It is interesting to note that value of $K_{\text{rel}}^{S_0}$ is much lower than of $K_{\text{TICT-S}_0}$ rate constant, which results in emerging of long-lived component with negative amplitude α_3 in the bleaching band range of ThT. Unfortunately, we could not directly monitor ThT molecules resided in nonrelaxed S_0* state, and it is not known why relaxation process in the ground state takes so long time. One of the possible hypotheses—a relaxation process may involve reversible ring-opening of the benzothiazole moiety. This may explain inability to detect ThT molecules in nonrelaxed S_0* state using our equipment (in this case absorption spectra will be shifted to the UV range) and the effect of viscosity on relaxation kinetics. Observation of effective photochemical reaction for ThT in chloroform also supports this hypothesis.

Conclusions

The results of transient absorption spectra dynamics revealed that upon ThT photoexcitation intramolecular charge transfer takes place leading to nonfluorescent TICT-state formation. The rate of this process is viscosity-dependent, and for low-viscosity solvents (water, alcohols) it is higher than 10^{11} s^{-1}. Therefore, intramolecular charge transfer is the main channel of the excited state deactivation for ThT in low-viscous media. The rate of the LE → TICT process significantly depends on viscosity and is comparable to the rate of solvent relaxation resulting in time-dependent Stokes shift of ThT gain band.

Spectral features of transient TICT state for ThT as well as parameters of its deactivation dynamics were reported for the first time. It was found that efficient nonradiative transition depopulates TICT-state and rate of this process depends significantly on solvent viscosity. Decay lifetime of TICT-state changed from 3.8 ± 0.1 ps (in H_2O) to 360 ± 60 ps (in butanol). We suggest that TICT-state deactivation process proceeds through conical intersection between TICT(S_1') and S_0 states.

The results obtained confirm the earlier proposed model[33,34] that twisted internal charge transfer process accompanied by torsional motion of benzothiazole and dimethylaminobenzene fragments of the molecule takes place in the excited state of the dye and ThT behaves as a molecular rotor.

Acknowledgment. This work was supported by Belarusian Republican Foundation for Fundamental Research (grants F10R-233, F09MC-046, X10R-227, F09-028). The authors are grateful to Dr. A. Ianoul for valuable discussions.

Supporting Information Available: Additional fitting results of transient absorption at several wavelengthes for ThT in low-viscous solvents, and image plot of transient absorption versus delay time and wavelength for ThT in butanol. This material is available free of charge via the Internet at http://pubs.acs.org.

References and Notes

(1) Selkoe, D. J. *Nature* **2003**, *426*, 900–904.
(2) Harper, J. D.; Lieber, C. M.; Lansbury, P. T., Jr. *Chem. Biol* **1997**, *4*, 951–959.
(3) Kelly, J. W. *Structure* **1997**, *5*, 595–600.
(4) Carrell, R. W.; Gooptu, B. *Curr. Opin. Struct. Biol.* **1998**, *8*, 799–809.
(5) Hashimoto, M.; Masliah, E. *Brain Pathol.* **1999**, *9*, 707–720.
(6) Koo, E. H.; Lansbury, P. T., Jr.; Kelly, J. W. *Proc. Natl. Acad. Sci. U. S. A.* **1999**, *96*, 9989–9990.
(7) Uversky, V. N.; Talapatra, A.; Gillespie, J. R.; Fink, A. L. *Med. Sci. Monitor* **1999**, *5*, 1001–1012.
(8) Uversky, V. N.; Talapatra, A.; Gillespie, J. R.; Fink, A. L. *Med. Sci. Monitor* **1999**, *5*, 1238–1254.
(9) Groenning, M. *J. Chem. Biol.* **2010**, *3*, 1–18.
(10) Naiki, H.; Higuchi, K.; Hosokawa, M.; Takeda, T. *Anal. Biochem.* **1989**, *177*, 244–249.
(11) Naiki, H.; Higuchi, K.; Matsushima, K.; Shimada, A.; Chen, W. H.; Hosokawa, M.; Takeda, T. *Lab. Invest.* **1990**, *62*, 768–773.
(12) LeVine, H. *Protein Sci.* **1993**, *2*, 404–410.
(13) LeVine, H. *Amyloid* **1995**, *2*, 1–6.
(14) LeVine, H. *Arch. Biochem. Biophys.* **1997**, *342*, 306–316.
(15) LeVine, H. *Methods Enzymol.* **1999**, *309*, 274–284.
(16) Allsop, D.; Swanson, L.; Moore, S.; Davies, Y.; York, A.; El-Agnaf, O. M.; Soutar, I. *Biochem. Biophys. Res. Commun.* **2001**, *285*, 58–63.
(17) Yoshiike, Y.; Chui, D. H.; Akagi, T.; Tanaka, N.; Takashima, A. *J. Biol. Chem.* **2003**, *278*, 23648–23655.
(18) Maskevich, A. A.; Stsiapura, V. I.; Kuzmitsky, V. A.; Kuznetsova, I. M.; Povarova, O. I.; Uversky, V. N.; Turoverov, K. K. *J. Proteome Res.* **2007**, *6*, 1392–1401.
(19) Sen, P.; Fatima, S.; Ahmad, B.; Khan, R. H. *Spectrochim. Acta A* **2009**, *74*, 94–99.
(20) Singh, P. K.; Kumbhakar, M.; Pal, H.; Nath, S. *J. Phys. Chem. B* **2010**, *114*, 2541–2546.
(21) Groenning, M.; Norrman, M.; Flink, J. M.; van de Weert, M.; Bukrinsky, J. T.; Schluckebier, G.; Frokjaer, S. *J. Struct. Biol.* **2007**, *159*, 483–497.
(22) Groenning, M.; Olsen, L.; van de Weert, M.; Flink, J. M.; Frokjaer, S.; Jorgensen, F. S. *J. Struct. Biol.* **2007**, *158*, 358–369.

(23) Raj, C. R.; Ramaraj, R. *Chem. Phys. Lett.* **1997**, *273*, 285–290.
(24) Dzwolak, W.; Pecul, M. *FEBS Lett.* **2005**, *579*, 6601–6603.
(25) Sabate, R.; Lascu, I.; Saupe, S. J. *J. Struct. Biol.* **2008**, *162*, 387–396.
(26) Kitts, C. C.; Vanden Bout, D. A. *J. Phys. Chem. B* **2009**, *113*, 12090–12095.
(27) Biancalana, M.; Makabe, K.; Koide, A.; Koide, S. *J. Mol. Biol.* **2009**, *385*, 1052–1063.
(28) Krebs, M. R.; Bromley, E. H.; Donald, A. M. *J. Struct. Biol.* **2005**, *149*, 30–37.
(29) Friedhoff, P.; Schneider, A.; Mandelkow, E. M.; Mandelkow, E. *Biochemistry* **1998**, *37*, 10223–10230.
(30) Voropai, E. S.; Samtsov, M. P.; Kaplevskii, K. N.; Maskevich, A. A.; Stepuro, V. I.; Povarova, O. I.; Kuznetsova, I. M.; Turoverov, K. K.; Fink, A. L.; Uverskii, V. N. *J. Appl. Spectrosc.* **2003**, *70*, 868–874.
(31) Singh, P. K.; Kumbhakar, M.; Pal, H.; Nath, S. *J. Phys. Chem. B* **2009**, *113*, 8532–8538.
(32) Dutta Choudhury, S.; Mohanty, J.; Upadhyaya, H. P.; Bhasikuttan, A. C.; Pal, H. *J. Phys. Chem. B* **2009**, *113*, 1891–1898.
(33) Stsiapura, V. I.; Maskevich, A. A.; Kuzmitsky, V. A.; Turoverov, K. K.; Kuznetsova, I. M. *J. Phys. Chem. A* **2007**, *111*, 4829–4835.
(34) Stsiapura, V. I.; Maskevich, A. A.; Kuzmitsky, V. A.; Uversky, V. N.; Kuznetsova, I. M.; Turoverov, K. K. *J. Phys. Chem. B* **2008**, *112*, 15893–15902.
(35) Lindgren, M.; Sorgjerd, K.; Hammarstrom, P. *Biophys. J.* **2005**, *88*, 4200–4212.
(36) De Ferrari, G. V.; Mallender, W. D.; Inestrosa, N. C.; Rosenberry, T. L. *J. Biol. Chem.* **2001**, *276*, 23282–23287.
(37) Tikhomirov, S. A.; Dubovski, V. L.; Kuzmitsky, V. A.; Stsiapura, V. I.; Maskevich, A. A. In *VII International conference on Laser Physics and Optical Technologies*; Kazak, N. S., Apanasevich, P. A., Kabanov, V. V., Kurilkina, S. N., Plavski, V. Y., Rusov, S. G., Eds. Minsk, 2008; Vol. 2, p 223−226.
(38) Singh, P. K.; Kumbhakar, M.; Pal, H.; Nath, S. *J. Phys. Chem. B* **2010**, *114*, 5920–5927.
(39) Blokhin, A. P.; Gelin, M. F.; Buganov, O. V.; Dubovskii, V. A.; Tikhomirov, S. A.; Tolstorozhev, G. B. *J. Appl. Spectrosc.* **2003**, *70*, 70–78.
(40) Marquardt, D. W. *J. Soc. Ind. Appl. Math.* **1963**, *11*, 431–441.
(41) O'Connor, D. V.; Phillips, D. *Time-correlated Single Photon Counting*; Academic Press: New York, 1984.
(42) Beechem, J.; Gratton, E.; Ameloot, M.; Knutson, J.; Brand, L. In *Topics in Fluorescence Spectroscopy* **2002**, 241–305.
(43) Knutson, J. R.; Beechem, J. M.; Brand, L. *Chem. Phys. Lett.* **1983**, *102*, 501–506.
(44) Levine, B. J.; Martinez, T. J. *Annu. Rev. Phys. Chem.* **2007**, *58*, 613–634.

JP105186Z